Topology and dynamics of the interaction between 5-nitroimidazole radiosensitizers and duplex DNA studied by a combination of docking, molecular dynamic simulations and NMR spectro...

ARTICLE *in* JOURNAL OF MOLECULAR STRUCTURE · APRIL 2011

Impact Factor: 1.6 · DOI: 10.1016/j.molstruc.2011.02.042

6 AUTHORS, INCLUDING:

Teodorico C. Ramalho
Universidade Federal de Lavras (UFLA)
188 PUBLICATIONS **1,685** CITATIONS
SEE PROFILE

Tanos C C França
Instituto Militar de Engenharia (IME)
63 PUBLICATIONS **411** CITATIONS
SEE PROFILE

Arlan Gonçalves
Federal Institute of Education Science and …
20 PUBLICATIONS **145** CITATIONS
SEE PROFILE

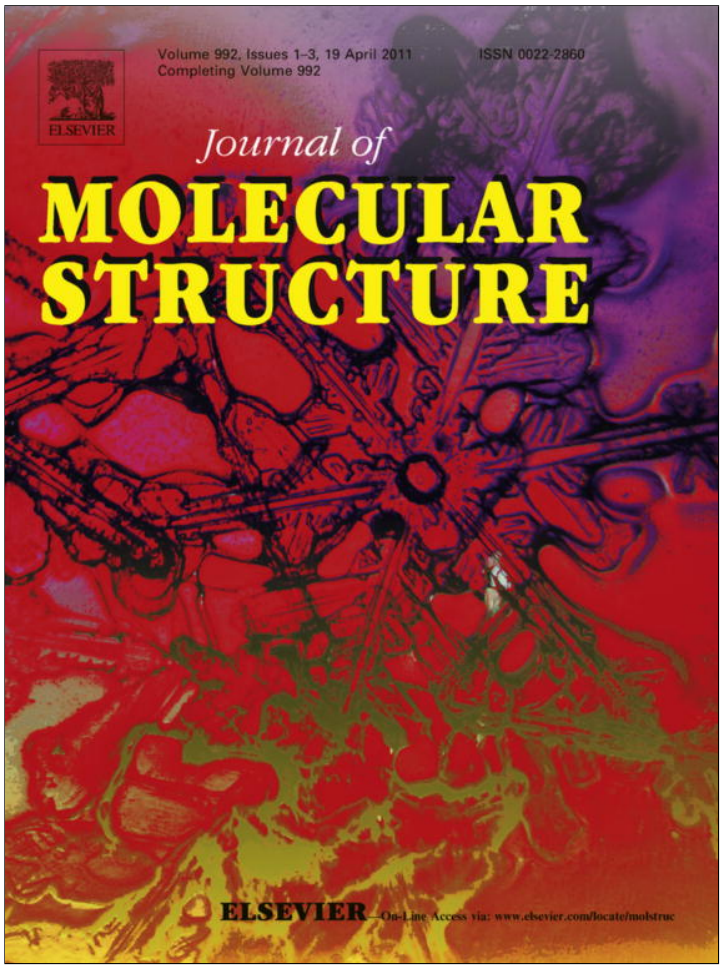

Journal of Molecular Structure 992 (2011) 65–71

Contents lists available at ScienceDirect

Journal of Molecular Structure

journal homepage: www.elsevier.com/locate/molstruc

Topology and dynamics of the interaction between 5-nitroimidazole radiosensitizers and duplex DNA studied by a combination of docking, molecular dynamic simulations and NMR spectroscopy

Teodorico C. Ramalho [a,*], Tanos C.C. França [b,2], Wilian A. Cortopassi [b,2], Arlan S. Gonçalves [c,3], Alan W.S. da Silva [d,4], Elaine F.F. da Cunha [a,1]

[a] Chemistry Department – Federal University of Lavras – Campus Universitário, 3037, 37200-000, Lavras, MG, Brazil
[b] Laboratory of Molecular Modeling Applied to the Chemical and Biological Defense – Military Institute of Engineering, Praça General Tibúrcio 80, 22290-270 – Rio de Janeiro/RJ, Brazil
[c] Chemistry Department – Federal Institute of Education Science and Technology, Estrada da Tartaruga, S/N°, CEP 29215-090 – Bairro Muquiçaba – Guarapari/ES, Brazil
[d] Department of Biochemistry, University of Cambridge, 80 Tennis Court Road, CB2 1GA, United Kingdom

ARTICLE INFO

Article history:
Received 19 December 2010
Received in revised form 15 February 2011
Accepted 18 February 2011
Available online 24 February 2011

Keywords:
Intermolecular interactions
PFG-NMR
Radiosensitizers

ABSTRACT

In spite of recent progress, cancer is still one of the most serious health problems of mankind. Recently, it has been discovered that tumor hypoxia can be exploited for selective anticancer treatment using radiosensitizers that are activated only under hypoxic conditions. The most commonly used radiosensitizers are the 5-nitroimidazole derivatives. The toxicity of bioreductive anticancer drugs, such as radiosensitizers is associated to their interaction with DNA. In this work, we have investigated the interaction between the model radiosensitizers metronizole, nimorazole and secnidazole with salmon DNA in order to get insights on the drug–macromolecule interactions. To this end, we have employed NMR techniques (PFG NMR spectra and spin–lattice relaxation rates) in combination with theoretical tools, such as docking calculations and MD simulations. Initially, results show that the δ values are not the most appropriated NMR parameters to map the interaction topology of drug–macromolecule complexes. Furthermore our data indicate that radiosensitizers, in the inactive form, interact considerably with DNA, significantly increasing its toxicity. In fact, we obtained a good agreement between that technique and docking and MD simulations. This suggests that improvements in the structures of these molecules in order to achieve new and more selective bioreductive anticancer drugs are still necessary.

1. Introduction

In spite of recent progress, cancer is still one of the most serious health problems of mankind. In particular, the capacity of destroying hypoxic cells in solid tumors has been one of the main deficiencies of anticancer chemotherapy. Recently, it has been discovered that tumor hypoxia can be exploited for selective anticancer treatment using radiosensitizers that are activated only under hypoxic conditions [1]. This was done by applying ^{1}H, ^{31}P and ^{19}F NMR/MRI of radiosensitizers for measuring tumor and tissue oxygenation [1]. Thus, normally inert compounds, which are activated by enzymes or by radiation under hypoxic conditions, will behave selectively toward tumors. Ideally, the compound should be reversibly reduced so that, in normal cells, it could readily revert to its inactive form [2–5]. In previous works, we have studied the physical chemistry properties associated with the biological activity of radiosensitizers in aqueous and carbon tetrachloride solution [6–10].

The most commonly used radiosensitizers are the 5-nitroimidazole derivatives (Fig. 1) [11,12], whose biological activity is related to their Electron Affinity (EA) and interaction with DNA [13–19]. In this way, radiosensitizers are bioreductive anticancer drugs activated by ionization radiation under hypoxic conditions. According to the action mechanism of this kind of drug, the activated form of radiosensitizers in solution interacts strongly with DNA and its neutral form does not. Actually, the interaction

Abbreviations: NMR, nuclear magnetic resonance; PFG, Pulse Field Gradient; EA, Electron Affinity; USP, University of São Paulo; MD, molecular dynamic; DOSY, diffusion ordered spectroscopy; RMSD, Random Mean Square Deviation; GAFF, General Amber Force Field; ACPYPE, AnteChamber PYthon Parser interface.

* Corresponding author. Tel.: +55 35 3829 1891; fax: +55 35 3829 1271.
E-mail addresses: teo@dqi.ufla.br (T.C. Ramalho), tanos@ime.eb.br (T.C.C. França), wiliancortopassi@gmail.com (W.A. Cortopassi), arlansgoncalves@gmail.com (A.S. Gonçalves), awd28@cam.ac.uk (A.W.S. da Silva), elaine_cunha@dqi.ufla.br (E.F.F. da Cunha).
[1] Tel.: +55 35 3829 1891; fax: +55 35 3829 1271.
[2] Tel.: +55 21 2546 7055; fax: +55 21 2546 7059.
[3] Tel.: +55 27 3362 6607.
[4] Tel.: +44 1223 766 018; fax: +44 1223 766 002.

0022-2860/$ - see front matter © 2011 Elsevier B.V. All rights reserved.
doi:10.1016/j.molstruc.2011.02.042

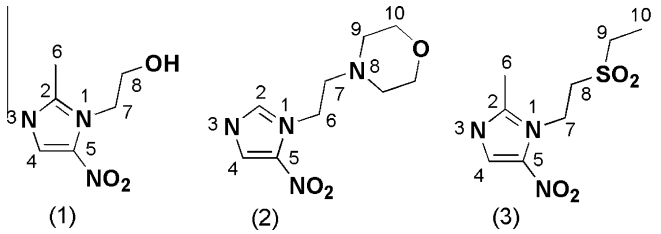

Fig. 1. Nitroimidazoles studied.

between the neutral form of a radiosensitizer and DNA increases its toxicity and leads to several collateral effects [20]. Therefore, the design of new and more selective radiosensitizers is quite dependent on the understanding of the nitroimidazole–DNA interaction. Surprisingly, in spite of the great importance of drug–DNA interaction studies, little computational and experimental work on radiosensitizer–DNA interactions has been seen in literature.

Thus, in this work, we used diffusion coefficients measured through Pulse Field Gradient (PFG) NMR experiments [21], together with MD simulations and docking studies in order to understand the interaction profile of some well known radiosensitizers with DNA.

2. Materials and methods

2.1. NMR experiments

All 5-nitroimidazoles were supplied by Rhodia Laboratories and by the Pharmacy Department of the University of São Paulo (USP) Brazil. The compounds **1**, **2** and **3** (metronidazole, nimorazole and secnidazole, respectively) are currently used in cancer treatment and can be considered model radiosensitizers [8].

PFG NMR spectra [22] were acquired at 27.0 ± 1 on a Bruker DRX-400 spectrometer using a 5 mm broad band inverse probe with a single gradient (*Z*). The spectra were obtained using solutions containing a mixture of radiosensitizers and salmon DNA at 110 μM, and were recorded with 32 scans with a recycle time of 1.5 s between scans. A pulse gradient bipolar stimulated echo sequence was used [21]. Diffusion coefficients were measured by incrementing the amplitude of the field gradient pulses in eight steps (0.68–17.03 G cm^{-1}).

Spin–lattice relaxation rates were measured with the inversion-recovery pulse sequence with the first relaxation delay varying from 12.0 to 32.0 s, depending on the sample concentration, and the second delay from 12.5 ms to 32.0 s. Nine points were used for each measurement. For non-selective measurements the 90° ^1H pulse length was 16 μs with 58 dB transmitter power (attenuation of 5 dB). For the selective experiments, the selective inversion pulse was achieved by replacement of the hard 180° pulse of the inversion-recovery sequence by a DANTE [23] train consisting of 300 identical hard pulses of the same nutation angle (0.6°) separated by 0.0001 ms delays with the transmitter power adjusted to 30 dB (28 dB attenuation in relation to the non-selective pulse) to give a selective 180° ^1H pulse length of 702.4 μs. All the reported relaxation rate results are the average of at least three measurements. In all cases, the relative uncertainty was of less than 20%, with most results having uncertainties lower than 10%. This procedure has been employed previously on similar systems with success [24].

2.2. Theoretical methods

The DNA strands used in this work, whose nucleotide sequence is presented in Fig. 2 correspond to the Dickerson dodecamer at

CGCGAATTCGCG
GCGCTTAAGCGC

Fig. 2. Nucleotide sequence of the dodecamer used in the present work.

1.65 Å of resolution deposited in the Protein Data Bank (PDB) [25,26] by Campbell et al. [27] under the code 2GVR. After downloaded from the PDB [25,26] this structure had its ligands manually removed and was docked with each ligand studied here using the software Molegro Virtual Docker® [28]. The compounds were docked between the DNA strands inside spheres with radius of 15 Å centered halfway between each strand and enclosing all the neighboring nucleotides in both strands. Due to the stochastic nature of the ligand–DNA docking search algorithm, about 10 runs were conducted and 30 docking solutions were retained for each ligand. The lowest energy poses obtained for each compound between the DNA strands were chosen for the further MD simulations steps.

The complexes formed between the lowest energy poses of each ligand inside the dodecamer were placed into water boxes containing about 17,700 water molecules and then submitted to energy minimization, with the amber force field *ff99SB* [29] implemented in the GROMACS 4.0 software [30], using the steepest descent algorithm followed by conjugate gradients and quasi Newton Raphson until reaching an energy gradient of 1.0 kcal mol^{-1} $Å^{-1}$. The subsequent MD steps were carried out according to the following procedure: First, 500 ps of MD at 300 K in the water molecules inside the box in order to allow for the equilibration of the solvent around the DNA strands. In this simulation, all DNA atoms had their positions restrained. Then, a full MD simulation of 8000 ps at 300 K with no restrictions was carried, using 1 fs of integration time and a cut-off of 14 Å (angstroms) for long-range interactions.

Because these DNA strands have only a residual net charge, which was balanced by contra-ions for these simulations, it was possible to use the direct cut-off for long-range interactions without smoothing functions. The effects of the electrostatic potential truncation are minor at 14 Å, and the cut-off procedure makes the calculations faster than other methods. Considering that the DNA strands and the water molecules inside the simulation box are composed by about 18,500 atoms, this method can save significant computational time.

Also, in order to obtain a neutral net charge for all the systems, the charges were neutralized by the addition of Na^+ ions. The program calculates the electrostatic potential to find best positions for ion insertion by replacing water molecules that are at least at 3.50 Å from the DNA surface. Periodic Boundary Conditions (PBC) were employed and the water model used was the Simple Point Charge water (SPC), the default solvent of the GROMACS 4.0 package [30].

To obtain the parameters and topologies for the referred compounds, we used AnteChamber PYthon Parser interfacE (ACPYPE) [31]. It is a tool based on Python programming language to use ANTECHAMBER (currently bundled in AmberTools version 1.4) [32] to generate parameters and topologies for chemical compounds and to interface with other python applications like CCPN tools [33] or ARIA2 [34]. ACPYPE is currently able to generate output files for the following MM softwares: CNS/XPLOR [35,36], GROMACS [30], CHARMM [37] and AMBER [29]. We used General Amber Force Field (GAFF) [38] parameters for the ligands and the atomic partial charges were calculated by the semi-empirical quantum chemistry program SQM [39] (via ANTECHAMBER) according to AM1-BCC parameters (parameterized to reproduce HF/6-31G* RESP charges). SQM was modified to include 6 decimals of precision instead of the default 3.

3. Results and discussion

3.1. NMR spectroscopy

NMR has been widely used for the characterization of ligand–receptor recognition processes [40,41], due to the advantage of the non-invasivity and non-alteration of the normal bio-functionality of the biomolecules under investigation. Moreover, many spectral parameters able to give both dynamical and structural information can be measured and analyzed (like chemical shift [41–43], relaxation rates and linewidth [44] and NOE [45]). In this line, we have used two different NMR experiments in order to get insights about interaction between some radiosensitizers and DNA. The NMR DOSY experiments were carried out in order to evaluate the intensity of interaction through the diffusion coefficient in the drugs–DNA complexes. The spin–lattice relaxation rates were determined aiming to identify the topology of the interaction between the studied drugs and DNA. Initially, the analysis was carried out using the diffusion coefficient values. For each case, the diffusion coefficient values were determined, and the results are summarized in Table 1.

For the studied solution, the average value of the diffusion coefficient in the presence of DNA is 1.98. This value is significantly lower than the diffusion coefficient value for the pure drug, which indicates a significant decrease of molecular diffusion of the studied drugs in the presence of salmon DNA. In fact, it is possible to say that the molecule now presents low diffusion coefficient values. This result strongly suggests that radiosensitizers in the neutral form are also forming a complex with the salmon DNA and the diffusion coefficient values are lower in the presence than absence of DNA. According to Table 1, compound **2** shows the strongest interactions with DNA followed by compounds **1** and **3**.

An identical conclusion is reached if the analysis is carried out using the overall average T_1^S values for the studied drugs. In fact, to study systems with fast conversion between the bound and free states, as is the case for the drug–macromolecule complexes, it has been demonstrated that selective spin–lattice relaxation rates (R_1^S) are more sensitive to the process than the non-selective spin–lattice relaxation rates (R_1^{NS}) [24]. In this line, we have performed our discussion in light of the T_1^S values. The absolute uncertainty of the T_1^S values was calculated according to standard procedures [46], and was always equal to or less than ±0.1. It is important to mention that only the average T_1^S values were used for all the isomers at the same concentration. Then, the same procedure was carried out using the overall average values for all the hydrogens.

Data from Table 2 show that the concomitant change in the chemical shift ($\Delta\delta$) values in the presence and absence of DNA is very small. Thus, as expected, the δ values are not the most appropriated NMR parameters to map the interaction topology of drug–macromolecule complexes. On the other hand, the spin–lattice relaxation rate variations (ΔT_1 values) are quite expressive. This result put clearly in evidence that there is a strong interaction between the studied radiosensitizers and the salmon DNA. On going from the values for the pure drugs to the values for drugs in the presence of DNA, the concomitant changes are small for δ results and large for T_1 data, up from −0.03 ppm to 4.8 s, respectively. Focusing now on the topology of the interaction in the drug–DNA complex, the hydrogen at position 4 of the imidazole ring, relative to the signal 7.9 (Fig. 1), was the most affected in the interaction process for all studied drugs. According to both NMR techniques used to characterize the interaction, we can observe that the compound **2** shows the strongest interaction with DNA followed by compounds **1** and **3**.

Table 1
Diffusion coefficients ($m^2\ s^{-1}$) of radiosensitizers in the absence and presence of salmon DNA.

Compounds	D_{alone}	$D_{with\ DNA}$	ΔD
1	3.65×10^{-11}	1.71×10^{-11}	1.94
2	3.62×10^{-11}	1.51×10^{-11}	2.11
3	3.52×10^{-11}	1.63×10^{-11}	1.89

Table 2
T1 values for compounds alone and interacting with DNA.

Compounds	Alone		with/DNA			
	Peak (ppm)	T_1^{alone} (s)	Peak (ppm)	$T_1^{with/DNA}$ (s)	$\Delta\delta$ (ppm)	$\Delta T_1{}^*$(s)
1	7.99	8.4	8.02	6.9	−0.03	1.6
	4.41	679.1	4.44	639.4	−0.03	39.7
	3.80	928.3	3.82	814.9	−0.02	113.4
	3.55	6.5	3.78	3.4	−0.02	3.1
	2.44	1.4	2.47	1.3	0.03	0.1
	1.12	6.1	1.15	4.5	0.03	1.6
2	7.99	7.2	7.99	2.4	0.00	4.7
	7.89	2.7	7.89	3.8	0.00	−1.1
	4.48	647.7	4.48	1.2	0.00	−1.2
	3.64	708.4	3.64	590.4	0.00	118.0
	2.75	628.2	2.75	481.7	0.00	146.5
	2.52	591.9	2.52	491.8	0.00	100.1
3	7.97	7.7	8.02	6.3	−0.05	1.4
	4.36	603.7	4.44	488.7	−0.07	115.0
	4.12	560.6	4.17	509.1	−0.05	51.5
	4.00	1.9	4.02	1.5	−0.02	0.4
	2.41	1.3	2.45	0.9.7	−0.04	0.3
	1.18	686.5	1.21	571.1	−0.03	115.4

* ΔT_1 (s) = T_1(alone) − T_1(with/DNA).

3.2. Theoretical results

In order to shed some more light on the experimental data of the overall interaction mechanism, we performed docking calculations and MD simulations. As expected, the diffusion coefficient values are lower in the presence than absence of DNA. Molecular modeling tools were employed to evaluate the 5-nitroimidazole-DNA interaction topology, showing good agreement between theory (docking energies) and experimental data (ΔD – variation of diffusion coefficients and T_1 measurements).

The calculation of partial atomic charges of each compound in Fig. 1 was carried out at the HF/6-311++G(d,p) level. The compounds were docked in the DNA binding site using the MVD® program [30]. Afterwards, the best fit for each compound was selected for the further MD simulation steps.

The docking data are in good agreement with the experimental NMR results obtained by both DOSY and Spin–lattice relaxation rate measurements. Table 3 shows that compound **2** displays the lowest docking energy followed by compounds **1** and **3**. The same tendency is observed in our experimental results (Tables 1 and 2). This rather good correlation demonstrates that the binding conformations and binding models of the studied radiosensitizers are reasonable. The docking stage shows that the hydrophobic portion of the binding site can accommodate many different sizes and shapes of hydrophobic moieties, while the specificity for basic drugs is conferred by interactions with the hydrophilic patch. In this context, the imidazole ring orientation governs the binding mode and the interaction with DNA. The results of spin–lattice relaxation rate variations reinforce that conclusion from the docking rationalization, because the highest ΔT_1 values were reached with hydrogen 4 in the imidazole ring (Fig. 1).

Now, in order to get more insight about the dynamics behavior of the drug–macromolecule complexes, some MD simulations were carried out. As described in the materials and methods sec-

Table 3
Docking energies (kJ mol^{-1}) of radiosensitizers in the absence and presence of salmon DNA.

Compound	Docking energy
1	−93.89
2	−101.05
3	−92.75

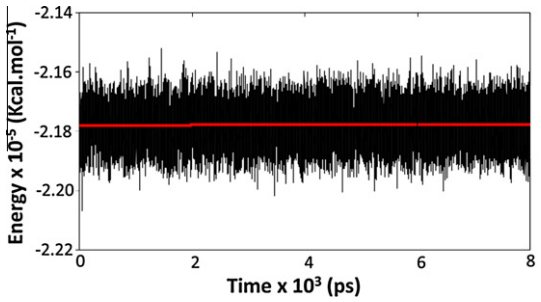

Fig. 3. Energy plot of the system DNA/compound **1** along the 8000 ps of MD simulation.

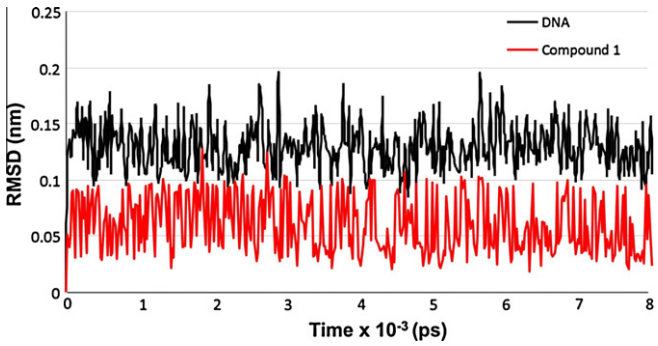

Fig. 4. RMSD plot for the system DNA/compound **1**.

tion, the energy minimized DNA strands docked with the lowest energy conformations of each ligand were submitted to 500 ps of position-restrained MD (PRMD) followed by 8000 ps of MD simulations with no restriction. The energy plots of each MD simulation show that the systems remained stable along the 8000 ps, with essentially no change in energy, as can be seen in the plot for compound **1** in Fig. 3.

Furthermore, temporal Random Mean Square Deviation (RMSD) calculations were carried out on all the atoms in the three systems DNA/Ligand for 8000 frames generated at each 1 ps of MD simulation. In this case, the result is a unique general value for each molecule monitored throughout the simulation time. Taking into account that the complexes could float inside the water box, each frame was adjusted to the former by the minimum squares method when calculating the standard deviation. In Fig. 4, where the variation of RMSD with time is monitored, it can be observed that the system DNA/compound **1** equilibrates along the first few picoseconds of the MD simulation. This behavior was common to all three MD simulations, with deviations never passing 0.2 nm. We also observed that, for all simulations, the temporal RMSD of the DNA strands alone, practically fits the temporal RMSD of the complexes (data not shown). Also, as expected, the ligands display a fluctuation greater than for the complexes but with a smaller RMSD, thus confirming the stability of the MD simulations.

In order to analyze and compare the dynamic behavior of each compound between the DNA strands along the MD simulations, we extracted one frame every 80 ps of simulation, totaling 100 frames for each system. These frames are shown in stick representations in Fig. 5. To make possible their visualization, only one frame of the DNA strands, represented in tube form, is shown in each case. Analysis of Fig. 5 shows that all the three ligands remained between the two DNA strands along the entire simulation time, close enough to the nucleotides to establish interactions.

An analysis of the interactions performed by each ligand with the DNA nucleotides along the MD simulations permitted to visualize that, despite remaining between the strands, none of them was able to perform and maintain H-bonds along all the simulation time, being stabilized only by electrostatic interactions. Compound **1** stayed in a pocket surrounded by the base pairs T = A and C = G above and A = T and T = A below, quite differently from compound **2** that presented a slight tendency to stabilize close to the pairs T = A and C = G above while compound **3** stayed in a pocket formed by the pairs T = A and A = T above.

Analyzing the dynamics behavior of each compound it was possible to realize that compound **2** was the most well behaved be-

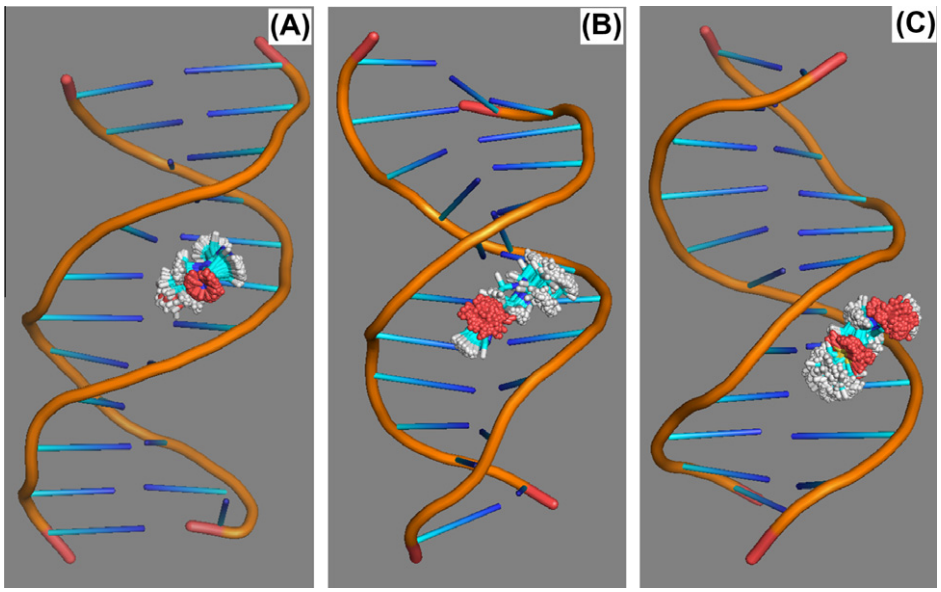

Fig. 5. Dynamical behavior of compounds **1** (A), **2** (B) and **3** (C).

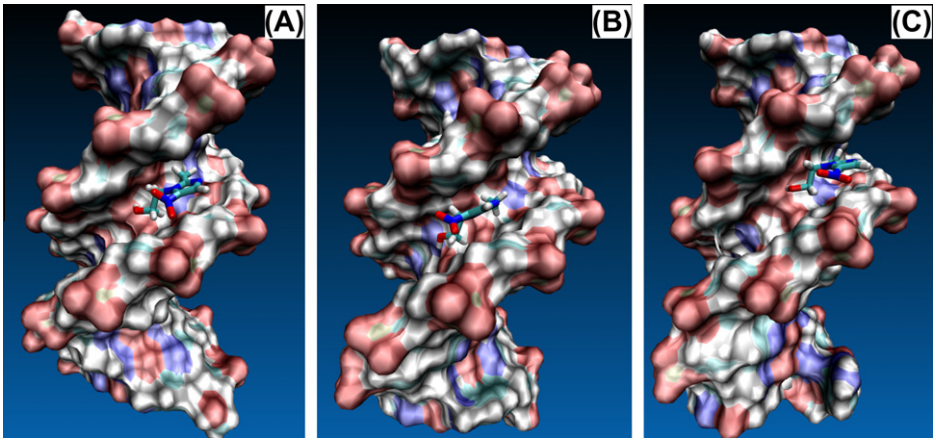

Fig. 6. Conformations of compound **1** inside the DNA cleft at 0000 ps (A), 4000 ps (B) and 8000 ps (C).

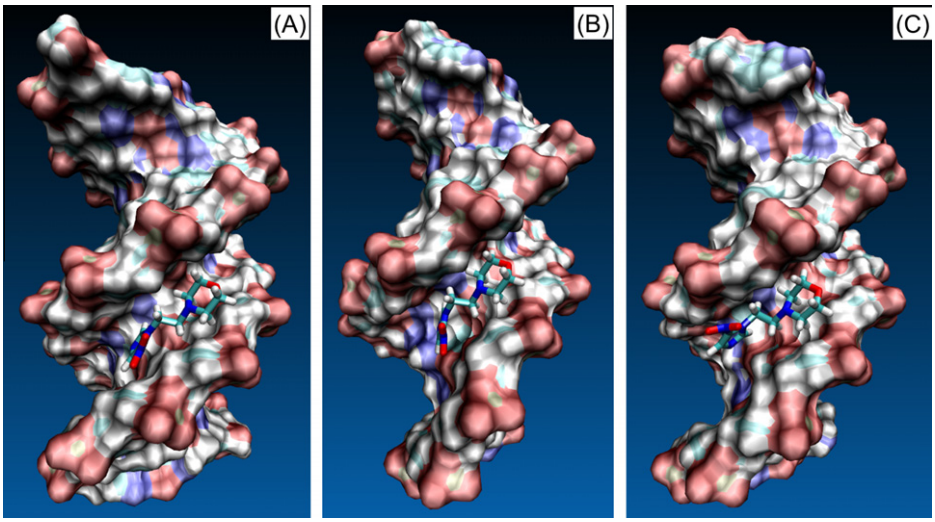

Fig. 7. Conformations of compound **2** inside the DNA cleft at 0000 ps (A), 4000 ps (B) and 8000 ps (C).

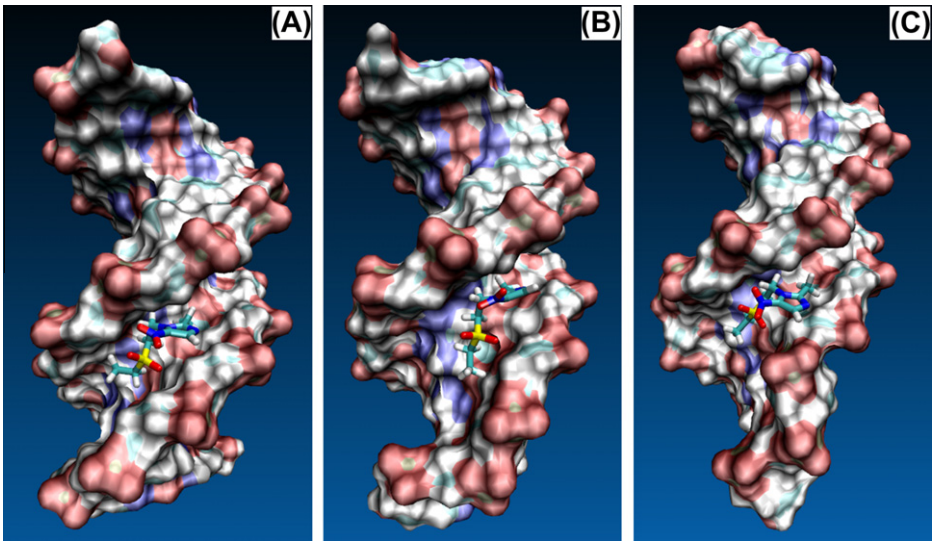

Fig. 8. Conformations of compound **3** inside the DNA cleft at 0000 ps (A), 4000 ps (B) and 8000 ps (C).

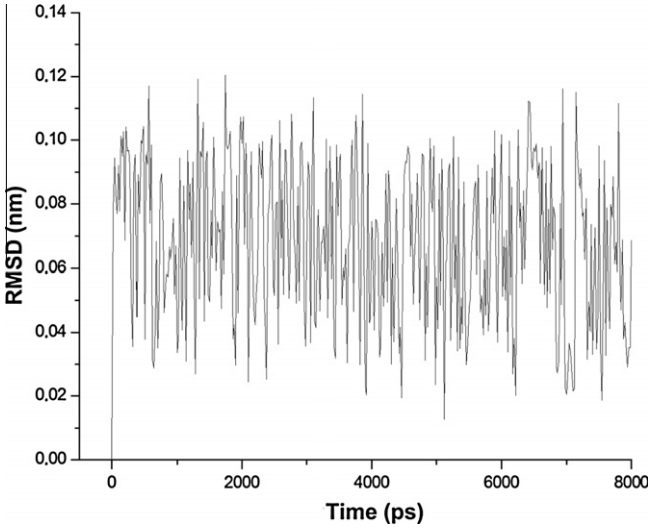

Fig. 9. Temporal RMSD of compound **1** along the MD simulation.

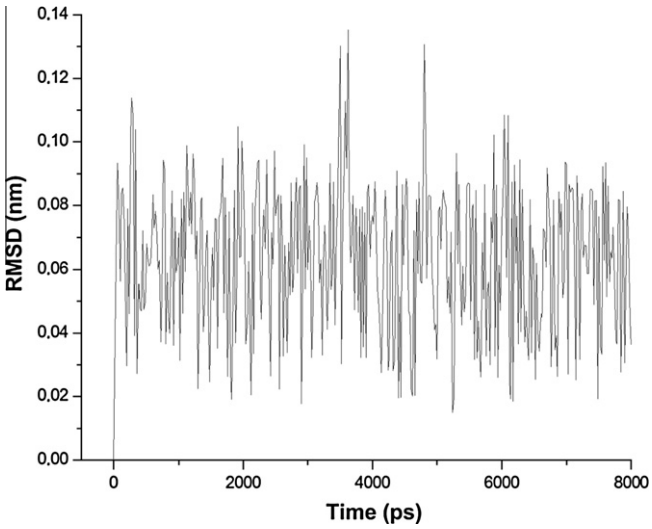

Fig. 10. Temporal RMSD of compound **2** along the MD simulation.

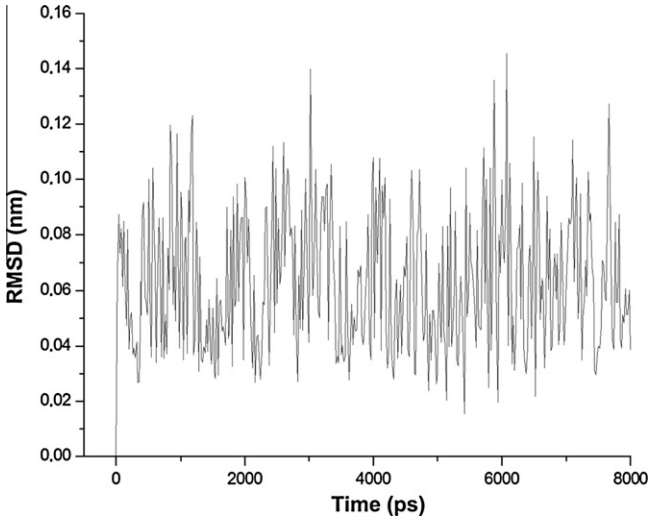

Fig. 11. Temporal RMSD of compound **3** along the MD simulation.

tween the strands, practically not changing its initial position along the 8000 ps, as can be seen in the illustrations of frames at times 0000, 4000 and 8000 ps for each compound in Figs. 6–9. The temporal RMSD plot in Fig. 10 shows that the deviation of compound **2** from its initial position remained most of the time under 0.1 nm. Compounds **1** and **3** deviation, on the other hand, exceeded 0.1 nm much more frequently (see Figs. 9 and 11). These results corroborate with the docking and experimental results reported here pointing out to compound **2** as able to establish stronger interactions with DNA than compounds **1** and **3**.

A possible reason to the better behavior of compound **2** could be its linear shape and the lesser freedom degree conferred to the molecule by the six membered ring. These features together could contribute to the ideal fitting of this molecule between the DNA strands.

It is well known that the EA of a radiosensitizer is responsible for 80% of its biological action [47,48], so that the radiosensitizer candidate compound should have lower EAs than oxygen [49]. On the other hand, compounds that present EA values which are too negative, have their redox properties significantly affected by the presence of small amounts of oxygen, resulting in a redox system known as futile cycle [1], thus leading to a loss of selectivity [1,49]. In this scenario, the imidazole ring has been identified as an essential pharmacophoric group that modulates that property. Therefore the interaction between DNA and the inactive form of a radiosensitizer will then be always present, significantly increasing its toxicity.

4. Conclusion

Herein, we have shown that DOSY NMR spectroscopy together with docking data can be a useful approach to evaluate the intensity of drug–macromolecule interaction. Furthermore, for the interaction topology, we have observed that the relaxation rate techniques, such as measurements of proton spin–lattice selective relaxation rates, represent a powerful tool to investigate the binding affinity of the ligand towards the receptor as well as the dynamical properties of ligand–protein complexes. Interestingly, we obtained a good agreement between that technique and MD simulations. It is clear from this study that those radiosensitizers in the neutral form show significant interaction with DNA. This conclusion could be useful to understand their toxicity mechanism. These data, together with other results [6–8], will allow the proposition of new and more selective bioreductive anticancer drugs.

Acknowledgments

Authors thank FAPEMIG, CNPq and FAPERJ for the financial support of this research. CNPq is also gratefully acknowledged for the fellowships and studentships. W.A.C. wishes to thank DMBranco (WAC) and Estudar Foundation (WAC) for the fellowships.

References

[1] S. Kasai, H. Nagasawa, M. Yamashita, Bioorg. Med. Chem. 9 (2001) 453.
[2] B.A. Teicher, Cancer Metastasis Rev. 13 (1994) 139.
[3] A. Tomida, T. Tsuruo, Anti-Cancer Drug Des. 14 (1999) 169.
[4] J.M. Brown, B.G. Wouters, Cancer Res. 59 (1999) 1391.
[5] T.C. Ramalho, T.C.C. Franca, M.N. Renno, A.P. Guimaraes, E.F.F. da Cunha, K. Kuca, Chem. Biol. Interact. 185 (2010) 73.
[6] T.C. Ramalho, R.B. de Alencastro, M.A. La-Scalea, J.D. Figueroa-Villar, Biophys. Chem. 110 (2004) 267.
[7] T.C. Ramalho, E.F.F. Cunha, F.C. Peixoto, J. Theor. Comp. Chem. 7 (2008) 37.
[8] T.C. Ramalho, M. Buhl, J.D. Figueroa-Villar, R.B. de Alencastro, Helvet. Chim. Acta 88 (2005) 2705.
[9] E.F.F. Cunha, R.B. Alencastro, T.C. Ramalho, J. Theor. Comp. Chem. 3 (2004) 1.
[10] T.C. Ramalho, M. Buhl, Mag. Reson. Chem. 43 (2005) 139.
[11] H. Hori, C.Z. Jin, M. Kiyono, S. Kasai, M. Shimamur, S. Inayama, Biorg. Med. Chem. 5 (1997) 591.

[12] J.D. Chapman, L.R. Coia, C.C. Stobe, E.L. Engelhart, M.C. Fenning, R.F. Schneider, Brit. J. Cancer 74 (1996) S204.
[13] R.C. Urtasun, M.B. Paliament, A.J. McEwan, J.D. Chapman, Brit. J. Cancer 74 (1996) S209.
[14] S. Claerhout, L. Verschooten, S. Van Kelst, R. De Vos, C. Proby, P. Agostinis, M. Garmyn, Int. J. Cancer. 127 (2010) 2790.
[15] S. Gonfloni, Oncogene 29 (2010) 6193.
[16] A. Yavlovich, B. Smith, K. Gupta, R. Blumenthal, A. Puri, Mol. Membrane Biol. 27 (2010) 364.
[17] A. Chiarini, J.F. Whitfield, R. Pacchiana, M. Marconi, U. Armato, I. Dal Pra, Oncol. Reports 23 (2010) 887.
[18] W.A. Denny, Expert Opin. Ther. Patents 15 (2005) 635.
[19] M. Ochsner, J. Photochem. Photobiol. B 39 (1997) 1–18.
[20] C.S. Platta, D. Khuntia, M.P. Mehta, Am. J. Clin. Oncol. – Cancer Trails 33 (2010) 398.
[21] B.F. Jordan, J. Peeterbroeck, O. Karroum, Cancer Lett. 293 (2010) 213.
[22] Y.C. Jean-Franc, M. Demeunynck, J. Garcia, J. Lhomme, Model. Biochem. 36 (1997) 4831.
[23] G. Bodenhausen, R. Freeman, G.A. Morris, Magn. Reson. 23 (1976) 171.
[24] M. Leone, E. Barile, J. Vazquez, A. Mei, D. Guiney, R. Dahl, M. Pellecchia, Chem. Biol. Drug Des. 76 (2010) 10.
[25] F.C. Bernstein, T. F Koetzle, G.J. Williams, E.E. Meyer, M.D. Brice, J.R. Rodgers, O. Kennard, T. Shimanouchi, M. Tasumi, J. Mol. Biol. 112 (1977) 535.
[26] H.M. Berman, J. Westbrook, Z. Feng, G. Gilliland, T.N. Bhat, H. Weissig, I.N. Shindyalov, P.E. Bourne, Nucleic Acids Res. 28 (2000) 235.
[27] N.H. Campbell, D.A. Evans, M.P.H. Lee, G.N. Parkinsona, S. Neidlea, Bioorg. Med. Chem. Lett. 16 (2006) 15.
[28] R. Thomsen, M.H. Christensen, J. Med. Chem. 49 (2006) 3315.
[29] V. Hornak, R. Abel, A. Okur, B. Strockbine, A. Roitberg, C. Simmerling, Proteins: Struct. Funct. Bioinformat. 65 (3) (2006) 712.
[30] B. Hess, C. Kutzner, D. van der Spoel, E. Lindahl, J. Chem. Theor. Comput. 4 (2008) 435.
[31] A.W. Sousa da Silva, W.F. Vranken, E.D. Laue, ACPYPE - AnteChamber PYthon Parser interfacE. Manuscript to be submitted. <http://acpype.googlecode.com> (accessed May 2010).
[32] J. Wang, W. Wang, P.A. Kollman, D.A. Case, J. Mol. Graph. Mod. 25 (2006) 247.
[33] W.F. Vranken, W. Boucher, T.J. Stevens, R.H. Fogh, A. Pajon, M. Llinas, E.L. Ulrich, J.L. Markley, J. Ionides, E.D. Laue, Proteins Struct. Funct. Bioinformat. 59 (2005) 687.
[34] W. Rieping, M. Habeck, B. Bardiaux, A. Bernard, T.E. Malliavin, M. Nilges, Bioinformatics 23 (2007) 381.
[35] A.T. Brunger, Nat. Protocols 2 (2007) 2728.
[36] C.D. Schwieters, J.J. Kuszewski, G.M. Clore, Prog. Nucl. Mag. Res. Spectrosc. 48 (2006) 47.
[37] B.R. Brooks, C.L. Brooks III, A.D. MacKerell Jr., L. Nilsson, R.J. Petrella, B. Roux, Y. Won, G. Archontis, C. Bartels, S. Boresch, A. Caflisch, L. Caves, Q. Cui, A.R. Dinner, M. Feig, S. Fischer, J. Gao, M. Hodoscek, W. Im, K. Kuczera, T. Lazaridis, J. Ma, V. Ovchinnikov, E. Paci, R.W. Pastor, C.B. Post, J.Z. Pu, M. Schaefer, B. Tidor, R.M. Venable, H.L. Woodcock, X. Wu, W. Yang, D.M. York, M. Karplus, J. Comp. Chem. 30 (2009) 1545.
[38] J. Wang, R.M. Wolf, J.W. Caldwell, P.A. Kollman, D.A. Case, J. Comp. Chem. 25 (2004) 1157.
[39] R.C. Walker, M.F. Crowley, D.A. Case, J. Comp. Chem. 29 (2008) 1019.
[40] M. Nomdedieu, A. Boudou, D. Georgescauld, E.J. Dufourc, Chem. Biol. Interact. 81 (1992) 243.
[41] L.Y. Lian, C.S. Allardyce, P.C.E. Moody, G.C.K. Roberts, Chem. Biol. Interact. 133 (2001) 13.
[42] L. Yiming, Q. Li, M. Sun, G. Song, S. Jiang, D. Zhua, Bioorg. Med. Chem. Lett. 14 (2004) 1585.
[43] S.G. Patching, A.R. Brough, R.B. Herbert, J.A. Rajakarier, P.J. Henderson, D.A. Middleton, J. Am. Chem. Soc. 126 (2004) 3072.
[44] S. Ravindranathan, J.M. Mallet, P. Sinay, G. Bodenhausen, J. Magn. Reson. 163 (2003) 199.
[45] A.P.R. Zabell, C.B. Post, Proteins 46 (2002) 295.
[46] C.D. Harris, Quantitative Chemical Analysis, W.H. Freeman and Company, New York, 1996.
[47] J.R. Pires, C. Saito, S.L. Gomes, A.M. Giesbrecht, A.T. Amaral, J. Med. Chem. 44 (2001) 3673.
[48] G. Chauviere, B. Bouteille, B. Enanga, C. Albuquerque, S.L. Croft, M. Dumas, J. Perie, J. Med. Chem. 46 (2003) 427.
[49] H. Horis, H. Nagasawa, H. Terada, Advances in Environmental Science and Technology: Oxidants in the Environment, Wiley, New York, 1994.